Millimeter-Scale Computing Platform for Next Generation of Internet of Things

Taekwang Jang, Myungjoon Choi, Yao Shi, Inhee Lee, Dennis Sylvester and David Blaauw

Dept. of Electrical Engineering and Computer Science, University of Michigan

Ann Arbor, USA

tkjang@umich.edu

(Invited Paper)

Abstract—The internet of things has enabled the communication of "smart" physical objects and improved the quality of machine service to humans. These achievements are based on the synergy of processing information collected by different sources. This trend will continue with the next class of computing platforms enabled by millimeter-scale sensors, diversifying the signal sources including biomedical, climate and surveillance targets. The key challenge of such systems is to achieve small die size, ultra-low power consumption, sufficient communication distance with the limited antenna size and accurate system duty-cycling.

Keywords — wireless sensor node; WSN; Internet of Things; IoT; Ultra-low power

I. INTRODUCTION

Innovations in communication technology have accelerated networking among existing and emerging computing platforms such as mobile hand-held devices, household electrical appliances and automobiles. By sharing and processing information gathered from the physical world, the quality of service can be improved, thus triggering economic benefit for the semiconductor circuit business referred to as the internet of things (IoT). However, most IoT applications have focused on the interactions among existing objects. Such networking can create appealing synergy, but make it difficult to create new paradigms of computation.

According to Bell's Law, a new class of computers with a smaller form factor is developed every decade, as shown in Fig. 1 and [1]. This trend has continued, with a progression from gigantic mainframes in 1960 to the current smart phones. With each change in computing platforms, the number of devices per person has also grown, opening wide the semiconductor market. Based on the extrapolation of this observed trend, we expect wide-spread use of mm-scale computing platforms for environmental monitoring, medical implants and surveillance in the next decade [2-4].

A mm-scale IoT sensor node offers a substantial advantage over its predecessors in terms of its potential proximity to the target object. For example, in electrocardiography (ECG) signal monitoring, a 2-cm separation of the electrodes of an implanted sensor node is sufficient to achieve a QRS peak amplitude of 5 mV, a value that is higher than that associated with the traditional approach of two patches applied to the neck
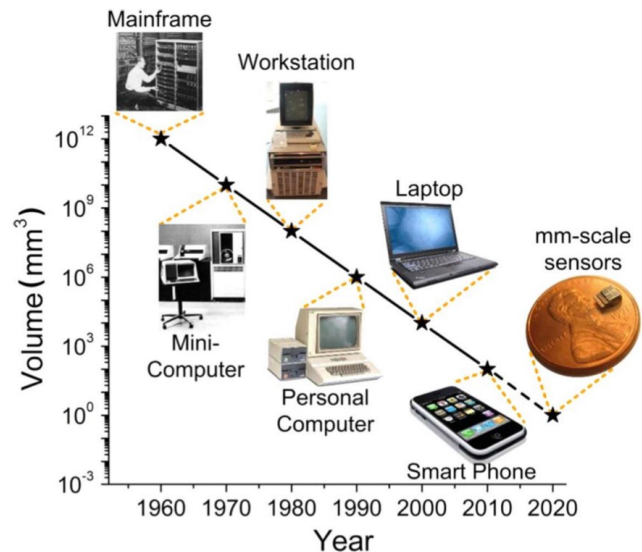

Fig. 1. Lifetime of various batteries according to the system power consumption

and wrist [5]. The implanted sensor node further benefits from noise isolation provided by the body to further improve the signal quality. Body-wearable solutions are typically susceptible to environmental noise, such as 60-Hz noise from power cables. Changes in humidity, temperature and body posture also affect the signal quality, causing low-frequency wandering [5]. Body implantation can dramatically reduce such low-frequency wandering and improve the robustness of the measurement system.

Another merit of mm-scale IoT sensor nodes is the mobility afforded by their small size and reduced weight. For example, [4] proposed an mm-scale imaging system with motion detection capability using a gradient-index rod lens. This millimeter form factor opens up the possibility of transport by bug-sized robots and unobtrusive deployment.

One of the key enablers of the mm-scale computing platform is the compact size achieved by continuous technology scaling and increased computational capability. The silicon fabrication technology has grown rapidly and approached single-digit channel lengths, which corresponds to a greater than 10x reduction in size of the silicon area compared with the 65-nm technology available in 2005 [5].
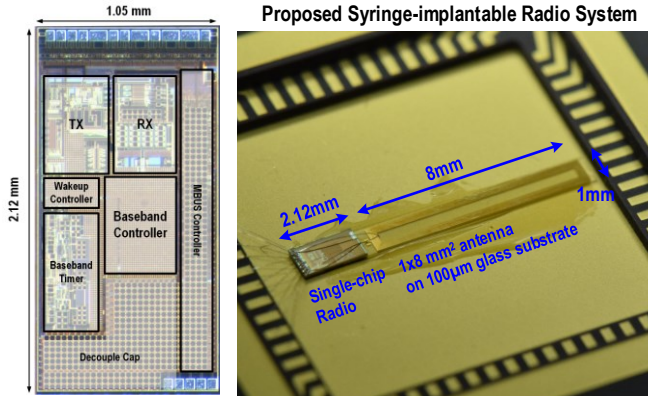
Fig. 2. Die photo and the system integration of the syringe injectable radio.

However, difficult challenges remain with respect to implementation of mm-scale IoT. Ultra-low power consumption is one of the main hurdle that must be overcome to reduce the form factor. Low-power circuit techniques can reduce the system energy budget and the battery capacity requirements, thereby reducing the form factor. Efficient wireless communication is also critical due to the limited battery capacity. The small antenna size makes wireless communication even more difficult. Further, the power management system is crucial due to the limited energy storage space. Energy harvesters using a solar cell or RF-DC converter can collect only nW to µW power in a mm-scale form factor. Therefore the harvester should remain efficient at very low power levels, which is challenging. In addition, an energy efficient DC-DC conversion circuit is mandatory; this can be realized by optimizing switching and conduction loss of switched-capacitor-based DC-DC converters. Efficient battery charging and circuit monitoring are also imperative to prevent battery stress and sustain long term system life cycle. Finally, an accurate and ultra-low power time management system is essential to maintaining synchronization with peers while sleeping to replenish energy. In this paper, we will summarize several recently published circuit techniques designed to resolve these aforementioned challenges.

II. WIRELESS COMMUNICATION

Monitoring biomedical signals plays a critical role in the realization of the IoT. ECG, bioimpedance, galvanic skin response and photoplethysmogram data are common bio-medical signals targeted by many implantable or wearable sensor nodes. For instance, an ECG provides useful information for the diagnosis of heart disorders and the implantation of sensor nodes. An implanted sensor node can provide continuous and accurate measurement of a signal of interest. However, implantation requires invasive surgery, which can limit the commercialization of such sensor nodes. A small, ultra-low power ECG monitoring system [2] enables syringe injection of the sensing platform, thus retaining the benefits of implantation, such as stable physical contact between the electrodes and the tissue, large signal strength and close proximity to the target organ, without requiring invasive surgery. The major obstacle of a syringe-injectable system is the small communication distance of the radio transceiver that results from the highly constrained antenna size, imposed by the syringe needle diameter. The work in [6] proposed an
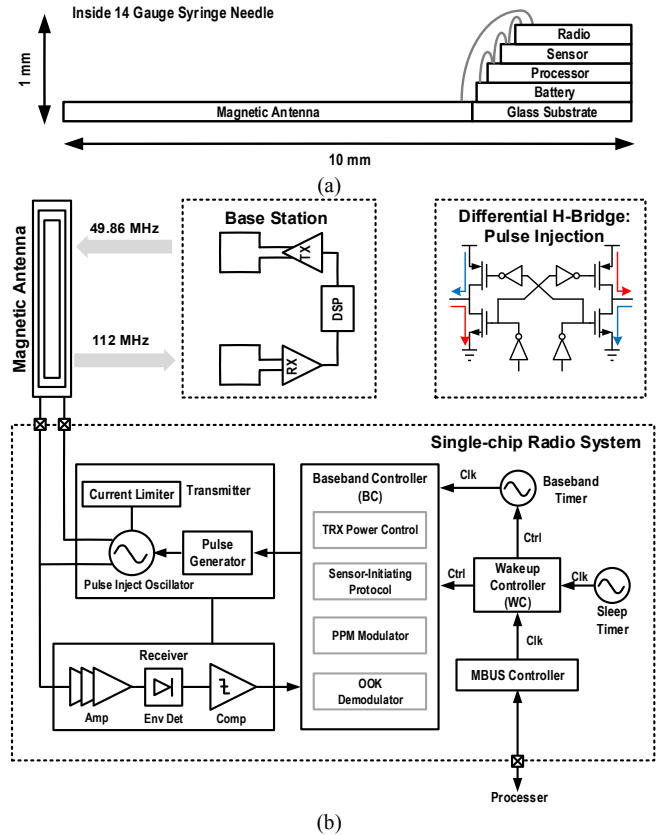

(a)

(b)

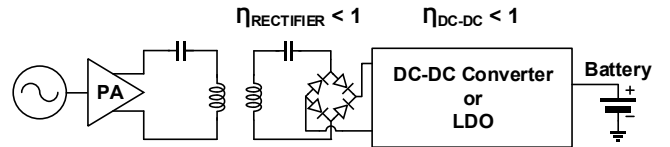Fig. 3. (a) Stack and (b) block diagram of the syringe injectable radio.

Fig. 4. Conventional voltage-mode wireless power transfer circuit.

energy efficient communication method using a 1-mm x 8-mm asymmetric magnetic antenna to achieve a 20-cm communication distance as shown in Fig. 2 and 3. A pulse-injection H-bridge LC oscillator and a proposed sensor-initiating synchronization protocol significantly improved its energy efficiency. However, the maximum current of the thin-film battery used in the proposed work is approximately 50 µA, which is insufficient to maximize the transmit efficiency. Therefore, [6] adopted a 1.3-nF on-chip capacitor as an energy-buffer that is continuously charged by the thin-film battery; a current limiter prevents overuse of current from the battery during the charging operation. This operation allows high peak transmitter current, but it comes at the expense of a long idle time to recharge the capacitor. However, the resulting pulse sparsity can be exploited using a pulse position modulation scheme. Each sensor node is assigned a unique pseudo-random interval pattern, which is sent as an identification header, followed by data in PPM format. The base-station detects the predefined pseudo-random interval of the header and accurately estimates the baseband timing offset of the sensor node. The local timer frequency is then adjusted to achieve synchronization.
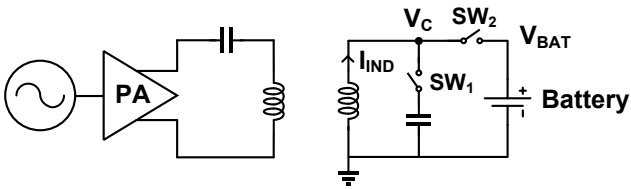
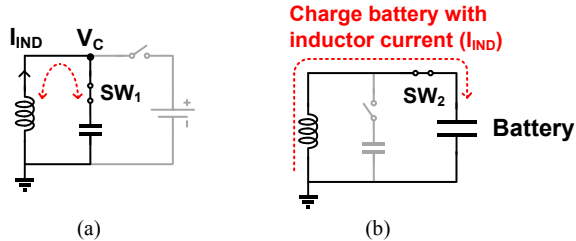Fig. 5. A current-mode resonant wireless power transfer circuit.

(a)   (b)

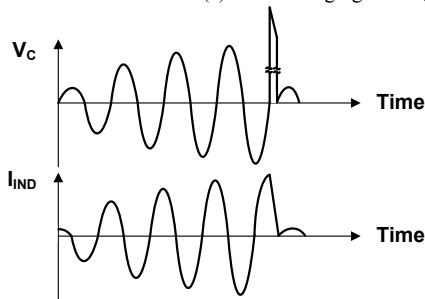Fig. 6. A receiver at resonance mode (a) and at charging mode (b).

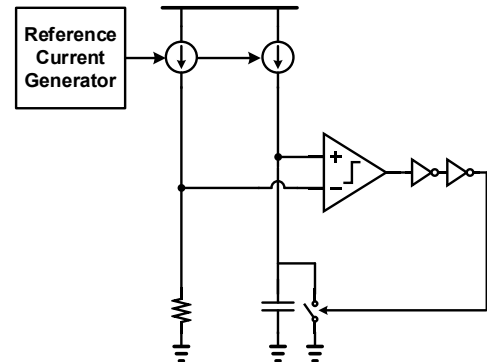Fig. 7. Transient waveforms of V_C and I_{IND}.

Fig. 8. Conventional relaxation oscillator using R-C time constant.

Fig. 9. A resistive frequency locking scheme using switched capacitor and a switched resistor.

III. WIRELESS POWER TRANSFER

Charging a wireless sensor node battery can be challenging because a wired connection to pads is impractical after the mm-scale sensor nodes are packaged. Thus, wireless power transfer is a popular option for charging a battery in such systems. Wireless power transfer has become increasingly popular for charging electric cars and handheld devices such as cellular phones. However wireless charging of mm-size sensor nodes has its own unique challenges: the small coil size associated with small sensor node form factor and the potential low incident power level on human tissue for implantable applications. These two constraints lead to small incident power on the receiver coil.

To overcome the issue of low power on the receiver coil, a recent work [7] introduced a current-mode resonant wireless power receiver and battery charger. Fig. 4 shows a conventional voltage-mode wireless power transmitter and a receiver. In this conventional scenario, any input power resulting in a receiver coil voltage amplitude less than the rectifier threshold voltage cannot be harvested. Furthermore, this method requires a two-step conversion: AC to DC rectification followed by DC to DC conversion. A rectifier and a DC-DC converter or a low dropout regulator are not ideal because each step introduces an efficiency loss. The output voltage also needs to be relatively accurate to safely charge a battery, increasing the design complexity and power overhead.

In contrast, a current-mode resonant wireless power receiver and charger, shown in Fig. 5, directly charges the battery with an inductor current in a boost converter fashion. This approach removes both the rectification and the DC-DC conversion steps. Fig. 6 shows receiver circuit configurations in two different modes: resonance and charging. In the resonance mode, the V_C amplitude increases as the LC tank resonates and accumulates energy. When the LC tank has stored enough energy, the circuit switches to its second mode, charging, where the inductor energy is transferred to the battery. The conceptual transient waveforms of V_C and I_{IND} are described in Fig. 7. The switch from resonance to charging occurs when V_C is 0 and rising, the point at which the inductor has all of the LC tank energy. The switching point from charging to resonance occurs when V_C is equal to V_{BAT} because at this point, the energy transfer is complete. It is also important to note that resonating for multiple cycles allows for balancing of switching and conduction losses, thus increasing power efficiency and lowering the minimum harvestable input power significantly.

IV. WAKE-UP TIMER

Millimeter-scale sensor nodes usually suffer from limited battery capacity due to their small form factor. Furthermore, the maximum harvestable energy is also limited in the nW- to µW-range, again due to the small size [8]. Therefore, such wireless systems are typically highly duty cycled to sustain their operation with a limited battery capacity and harvested

energy. The system sleeps for a long time to save or harvest energy and then wakes up to collect and process the data which it then periodically sends out using the radio. In this system scenario, it is critical to minimize the sleep power, which is typically dominated by the always-on wake-up timer. In addition, synchronization with peers requires additional overhead energy. The timer in each sensor node has timing uncertainty caused by the temperature, supply voltage differences and intrinsic noise. As a consequence, each sensor node wakes up at a different time. Therefore, a sensor must send radio signals until its peer responds to achieve synchronization, thereby wasting energy.

Wake-up timers that use a resistive frequency locked loop [9][10] represent a good circuit topology for satisfying the power and accuracy requirements, as shown in Fig. 8. Conventional R-C oscillators directly switch an R-C core to generate the output frequency, as shown in Fig. 9. In this structure, the clock period is affected by the temperature-sensitive comparator delay. Thus it requires a power-hungry comparator in order to make its delay negligible compared with the overall period. On the other hand, a resistive frequency locked loop uses a switched capacitor to sense the oscillation frequency of the voltage-controlled oscillator and then compares the resistance of the switch capacitor to a temperature compensated resistor. This approach ensures that there are no delay elements contributing to the oscillation period, thus achieving an excellent temperature coefficient while maintaining ultra-low power consumption. The work in [10] demonstrated power consumption of 4.7 nW while maintaining a frequency inaccuracy of less than 20 ppm/°C.

V. Conclusion

In this paper, we gave an overview of the challenges and mitigating circuit techniques for mm-scale computing platforms targeting the next generation of the IoT. Achieving ultra-low power consumption, wireless communication topology and energy efficient power and timing management are key challenges that must be overcome to improve the performance and sustainability of a mm-scale system.

References

[1] Bell, G., "Bell's Law for the Birth and Death of Computer Classes", Trans. Roy. Soc. London, vol. A247, pp. 529–551, April 1955. *(references)*

[2] D. Jeon, *et al.*, "24.3 An implantable 64nW ECG-monitoring mixed-signal SoC for arrhythmia diagnosis," in *IEEE ISSCC,* Feb. 2014 pp.416-417.

[3] Y. Lee, *et al.*, "A Modular 1 mm^3 Die-Stacked Sensing Platform With Low Power I^{2}C Inter-Die Communication and Multi-Modal Energy Harvesting," *IEEE JSSC*, vol. 48, no. 1, pp. 229-242, Jan. 2013.

[4] G. Kim, *et al.*, "A millimeter-scale wireless imaging system with continuous motion detection and energy harvesting," in *IEEE VLSI-C,* June. 2014, pp. 1-2.

[5] International technology roadmap for semiconductors, 2014.

[6] Y. Shi et al., "A 10mm3 syringe-implantable near-field radio system on glass substrate," *IEEE ISSCC,* Feb. 2016, pp. 448-449.

[7] M. Choi, et al., "A current-mode wireless power receiver with optimal resonant cycle tracking for implantable systems," *IEEE ISSCC,* Feb. 2016, pp. 372-373.

[8] I. Lee, et al., "A >78%-efficient light harvester over 100-to-100klux with reconfigurable PV-cell network and MPPT circuit," *IEEE ISSCC*, Feb. 2016, pp. 370-371.

[9] M. Choi, *et al.*, "A 99nW 70.4kHz Resistive Frequency Locking On-Chip Oscillator with 27.4ppm/ºC Temperature Stability ," in *IEEE VLSI-C*, June. 2015, pp. C238-C239.

[10] T. Jang, et al., "A 4.7nW 13.8ppm/¿¿C self-biased wakeup timer using a switched-resistor scheme," in *IEEE ISSCC*, Feb. 2016, pp. 102-103.